Biochimica et Biophysica Acta, 1153 (1993) 23–33
© 1993 Elsevier Science Publishers B.V. All rights reserved 0005-2736/93/$06.00

BBAMEM 76132

Hepatoselective carrier-mediated sodium-independent uptake of pravastatin and pravastatin-lactone

Kornelia Ziegler * and Silke Hummelsiep

Institut für Pharmakologie und Toxikologie der Justus-Liebig Universität, Frankfurterstr. 107, 35392 Giessen (Germany)

(Received 23 March 1993)
(Revised manuscript received 13 July 1993)

Key words: HMG-CoA reductase inhibitor; Pravastatin; Transport; Liver; Bile acid; (Rat)

Pravastatin and pravastatin-lactone are not taken up into extrahepatic cells such as fibroblasts, or hepatoma cells such as AS-30D ascites hepatoma cells or FAO cells. In contrast, pravastatin is taken up into isolated rat hepatocytes by a carrier mediated, saturable, temperature-dependent and energy-dependent mechanism. The kinetic parameters for the saturable uptake are K_m 27 μM, V_{max} 537 pmol/mg per min. The permeability coefficients were determined to be $9.829 \cdot 10^{-7}$ cm/s at 4°C, $1.76 \cdot 10^{-6}$ cm/s at 7°C, $3.85 \cdot 10^{-6}$ cm/s at 17°C and $5.82 \cdot 10^{-6}$ cm/s at 37°C. The activation energy is 60 kJ/mol for 100 μM pravastatin at 37°C. The Q_{10} values are between 1.7 and 2.8. In the presence of metabolic inhibitors and in the absence of oxygen, transport is inhibited. Uptake of pravastatin is not dependent on an extracellular to intracellular sodium-gradient. Replacement of chloride by sulfate, nitrate, gluconate or thiocyanate significantly inhibits the uptake of pravastatin. Uptake is competitively inhibited by cholate and taurocholate in the presence and absence of sodium. Pravastatin, however, competitively inhibits the uptake of cholate and taurocholate only in the absence of sodium. In addition, pravastatin-lactone enters liver cells via an energy-dependent, carrier-mediated uptake system. For the saturable energy-dependent part of the hepatocellular uptake a K_m value of 9 μM and a V_{max} value of 621 pmol/mg per min was determined. The permeability coefficient of pravastatin-lactone uptake is calculated to be $5.41 \cdot 10^{-6}$ cm/s at 37°C. The uptake of pravastatin-lactone is competitively-noncompetitively inhibited by pravastatin and by lovastatin and vice versa. These results indicate that the hepatoselectivity of pravastatin is due to its carrier-mediated uptake into rat hepatocytes via a sodium-independent bile acid carrier. Pravastatin-lactone resembles pravastatin-sodium in its hepatoselectivity.

Introduction

The recent development of specific competitive inhibitors of 3-hydroxy-3-methylglutaryl coenzyme A (HMG-CoA) reductase, the key enzyme that regulates cholesterol synthesis, has provided an important new therapeutic approach to the treatment of hypercholesterolaemia [1–3]. The target organ for HMG-CoA reductase inhibitors, such as pravastatin [4–6] and lovastatin [7,8], is the liver, since the liver is both the major site of lipoprotein production and low density lipoprotein catabolism [9]. The possibility of deleterious side effects of HMG-CoA reductase inhibitors in therapeutic situations depends in part upon the degree to which these agents exert their inhibitory influence in extrahepatic tissues [10–12]. Data on the relative rates of uptake of pravastatin and lovastatin by the liver and peripheral tissue are contradictory [5,6,13,14]. For lovastatin and other hydrophobic compounds, e.g. simvastatin and mevastatin, which are administered orally as lactones [15], extrahepatic side effects [16,17] and the uptake into extrahepatic tissues have been described [4,5]. The greater hepatoselectivity of pravastatin, which is administered as the open acid [18], compared to lovastatin is the result of the higher hydrophilicity of the compound [19,20] and, as shown recently in a study from our laboratory, is due to its affinity to a sodium-independent bile acid transporter [21]. This transport system exists predominantly in the basolateral membrane of liver cells [22]. It is responsible for the rapid extraction of pravastatin from the circulation thereby preventing suppression of cholesterol synthesis in extrahepatic organs. This conclusion was based on indirect measurements using unlabelled open acid pravastatin [21]. The aim of the present investigation was therefore the evaluation of the cell specificity of pravastatin-sodium and the characterization of the mechanisms of the uptake of the open acid ^{14}C-labelled pravastatin into isolated rat hepatocytes.

Corresponding author.

Furthermore, we studied the uptake mechanisms of ^{14}C-labelled pravastatin-lactone to see whether the lactone differs in its kinetic behaviour and tissue distribution compared to the open acid. Part of the results have been presented in preliminary form [23].

Materials and Methods

Materials

Pravastatin, pravastatin-lactone, [^{14}C]pravastatin (spec. act. 13 mCi/mmol) and [^{14}C]pravastatin-lactone (spec. act. 10 mCi/mmol) and lovastatin were gifts of Bristol-Myers Squibb (Munich, Germany). The chemical structure of the compounds is given in Fig. 1. Collagenase was purchased from Boehringer, Mannheim, Germany, cholate sodium salt, taurocholate, bromosulfophthalein (BSP) were from Serva, Heidelberg, Germany, bumetanide was a gift of Prof. Petzinger, Giessen, Germany.

All other chemicals used were of the highest purity grade available commercially.

Methods

Isolation of rat hepatocytes. Rat liver cells were isolated from male Wistar rats (body weight 200–260 g) by recirculating collagenase perfusion according to the method of Berry and Friend [24]. After 30 min of equilibration in Tyrode buffer (137 mM NaCl, 2.7 mM KCl, 1.05 mM $MgCl_2$, 12 mM $NaHCO_3$, 5.55 mM glucose, 0.42 mM NaH_2PO_4), pH 7.4 at 37°C in carbogene atmosphere (95% O_2/5% CO_2), the viability of the cells was tested by the Trypan blue exclusion test [25]. The contamination with non-parenchymal cells was less than 1.5% as determined by light microscopy. All experiments were performed within 2 h after isolation with a hepatocyte suspension containing more than 80% viable cells under incubation conditions mentioned above.

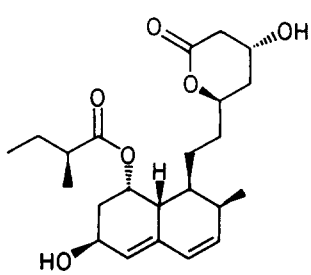

Pravastatin-lactone

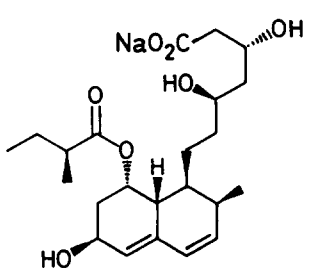

Pravastatin-Na

Fig. 1. Chemical structure of pravastatin and pravastatin-lactone.

Isolation of AS-30D ascites hepatoma cells, FAO cells and fibroblasts. The transplantable AS-30D ascites hepatoma cell line was carried in female Sprague-Dawley rats. The tumor cells were transplanted at weekly intervals by intraperitoneal injection of 0.5 ml ascites fluid. For uptake studies, tumor cells were collected and washed in Tyrode buffer. FAO cells and fibroblasts were kindly provided by Dr. J. Doehmer, TU Munich, Germany.

Transport studies. The uptake of [^{14}C]pravastatin and [^{14}C]pravastatin-lactone was measured using a liver cell suspension containing $2 \cdot 10^6$ cells/ml, or a suspension of AS-30D ascites hepatoma cells, FAO cells or fibroblasts containing $10 \cdot 10^6$ cells/ml; this corresponds to 4 mg of cell protein as determined by Bradford reagent [26].

1 ml of the cell suspensions was incubated with 3.4 μM [^{14}C]pravastatin or 2.7 μM [^{14}C]pravastatin-lactone and increasing concentrations of unlabelled pravastatin or pravastatin-lactone at 37°C. Uptake of the substrates was terminated by centrifugation of 100 μl aliquots of the cell suspensions at the times indicated in the figure legends through a silicon oil layer using a Beckman Microfuge B. The radioactivity taken up into the cell pellet was determined by liquid scintillation counting after addition of Ecco plus 2000 (Roth, Karlsruhe, Germany) in a Raytest 4700 counter (Straubenhardt, Germany).

For determination of the temperature dependence of uptake, the initial uptake rate of the substrates was measured at 7, 17, 27 and 37°C in Tyrode buffer after preincubation of the cell suspensions for 10 min at the desired temperatures.

Energy dependence was evaluated by incubation of the cells in the absence of oxygen (preincubation for 30 min in the presence of N_2/CO_2) as described [29] or after preincubation with metabolic inhibitors as indicated in the legends to the corresponding figures.

Sodium dependence of uptake was studied in sodium-free-Tyrode buffer, in which sodium was replaced by lithium, choline, potassium or *N*-methylglucamine. After a 30 min equilibration of the hepatocytes in sodium-Tyrode buffer, cells were washed twice in the appropriate sodium-free-Tyrode buffer.

Membrane potential dependence of uptake was measured in a Tyrode buffer in which chloride was replaced by sulfate, nitrate, thiocyanate or gluconate.

After 30 min equilibration in Tyrode buffer, cells were washed twice in the appropriate chloride-free Tyrode buffer. Initial uptake rates were determined.

In the case of inhibition studies, the inhibitors were added 30 s prior to the cell suspensions. Initial uptake rates were determined and plotted according to Lineweaver and Burk [29], Woolf-Hofstee [30] or Cornish-Bowden [31] to determine the type of uptake inhibition. K_i values were determined according to Dixon [32].

Thin-layer-chromatography analysis of [^{14}C]-pravastatin and [^{14}C]pravastatin-lactone metabolites. Isolated hepatocytes were incubated in Tyrode buffer containing 0.1 μCi of radiolabelled pravastatin or pravastatin-lactone. Aliquots of 100 μl were withdrawn after definite intervals over 1 h. The cells were centrifuged through silicon oil. Samples of 70 μl of the incubation buffer were applied onto thin-layer chromatography plates and chromatographed in a solvent system of 85% dichlormethan/15% methanol for pravastatin-lactone and methanol/water/acetic acid/triethylamine (450:550:1:1, v/v) for pravastatin-sodium. Radioactivity was detected using a Radio-TLC-Analysator from Raytest (Straubenhardt, Germany).

Statistical methods. All experiments were performed at least three times. The results are expressed as mean ± S.D. The plots mentioned above were calculated by linear regression analysis, the IC_{50} values by logarithmic regression analysis. Kinetic parameters were calculated using the program BMDPAR (derivative-free nonlinear regression analysis) on a Cyber 960 computer. The following equation was used:

$$V_o = (V_{max} \cdot S/(K_m + S)) + P \cdot S$$

Statistical significance was tested by a two factorial variance analysis with the program BMDP 2V on a CDC Cyber 960 computer.

Results

Cell specificity of the uptake of pravastatin and pravastatin-lactone

Pravastatin and pravastatin-lactone are not accumulated into AS-30D ascites hepatoma cells, FAO cells or fibroblasts (Fig. 2A and Fig. 2B). In the case of pravastatin the uptake rates were 600 pmol/mg per min for isolated rat liver cells, 2 pmol/mg per min for AS-30D ascites hepatoma cells, 90 pmol/mg per min for FAO cells and 10 pmol/mg per min for fibroblasts at a pravastatin concentration of 100 μM. In the case of pravastatin-lactone uptake rates were 1053 pmol/mg per min for hepatocytes, 2 pmol/mg per min for AS 30D ascites cells and 10 pmol/mg per min for fibroblasts. In addition, these cells are not able to transport bile acids [33].

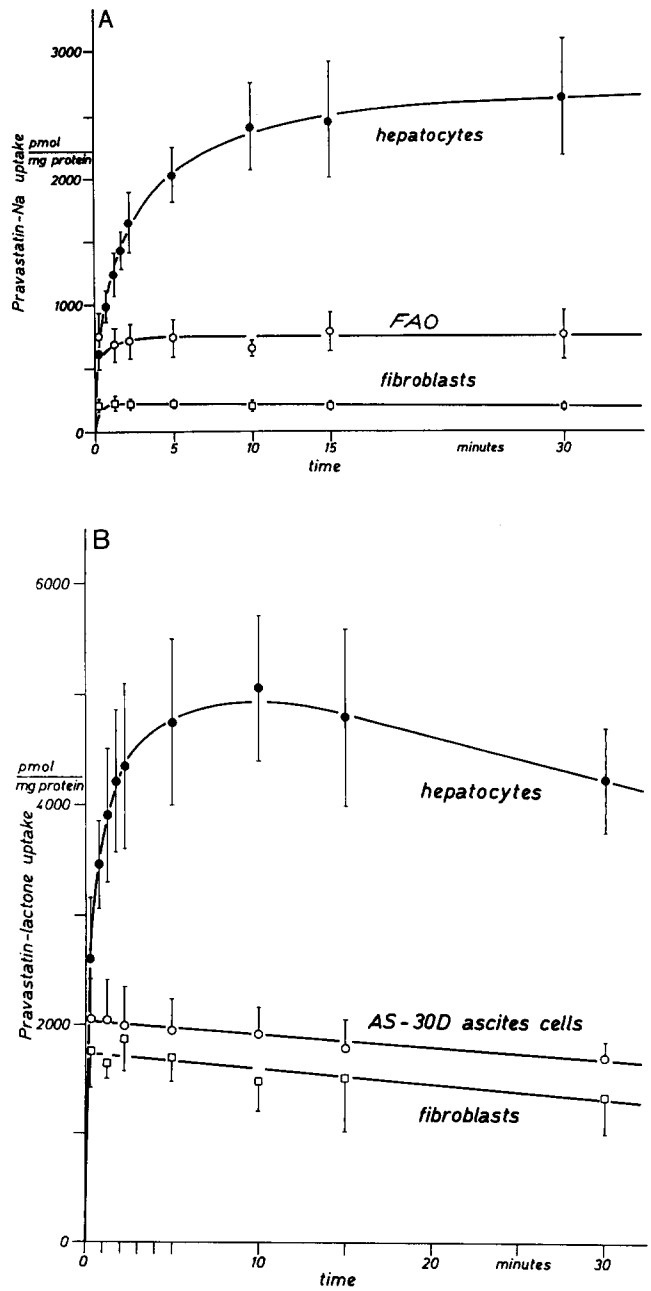

Fig. 2. Cell specificity of pravastatin and pravastatin-lactone uptake. The uptake of pravastatin (A) and pravastatin-lactone (B) was measured into isolated rat hepatocytes (●), AS30D ascites hepatoma cells (Fig. 2B ○), FAO cells (Fig. 2A ○) and fibroblasts (□). The concentration of pravastatin and pravastatin-lactone used were 100 and 135 μM, respectively. All cell suspensions correspond to a protein concentration of 4 mg/ml medium. $n = 3$; means ± S.D.

Uptake kinetics of pravastatin and pravastatin-lactone

Pravastatin is taken up by rat liver cells in a time- (Fig. 2A) and concentration-dependent manner (Fig. 4). The uptake rate is linear for 105 s. This linear part of uptake is referred to as initial uptake velocity.

Time-dependent saturation is reached after 30 min. 90% of pravastatin accumulated into rat hepatocytes after 30 min of incubation is found in the cytosol, whereas 10% is found in the membrane fraction after disruption of the cells and 100000 × g centrifugation (data not shown). Pravastatin is accumulated into the cells 79 times the extracellular concentration at an extracellular concentration of 3.4 μM and 25 times at 100 μM. The cellular concentration does not decrease until 60 min of uptake. At that time, in the supernatant of cell suspensions incubated with pravastatin, most of the radioactivity is associated with the native compound (Fig. 3).

The plot of V_i for different substrate concentrations shows a curvilinear dependence on pravastatin concentration (Fig. 4). At higher concentrations pravastatin uptake occurs in part by diffusion. Permeability coefficients of $9.8 \cdot 10^{-7}$ cm/s at 4°C, $1.7 \cdot 10^{-6}$ at 7°C, $3.8 \cdot 10^{-6}$ at 17°C and $5.8 \cdot 10^{-6}$ at 37°C could be calculated. By computer analysis of the data using the program BMDPAR a K_m of 27 μM and a V_{max} of 537 pmol/mg per min was calculated. Transforming the data according to Lineweaver and Burk provided identical results (Fig. 5). Plotting the data of the carrier-mediated part of pravastatin uptake according to Woolf-Hofstee it becomes evident that only one transport system for pravastatin exists at the plasma membrane of liver cells (Fig. 6). Pravastatin-lactone is accumulated into liver cells 73-fold over the extracellular concentration at an extracellular concentration of 2.7 μM and 22-fold at 135 μM. After 5 min of uptake cellular concentration of pravastatin-lactone rapidly decreases (Fig. 7). Several metabolites could be detected in the supernatant of those cell suspensions by TLC (Fig. 8). After 60 min of uptake radioactivity in the supernatant is associated totally with a metabolite, which was not further characterized.

In the case of pravastatin-lactone the permeability coefficient was calculated to be $5.41 \cdot 10^{-6}$ cm/s. For the saturable part of uptake a K_m value of 9 μM and V_{max} of 621 pmol/mg per min was determined (Fig. 9). As is evident from the Lineweaver-Burk plot and the

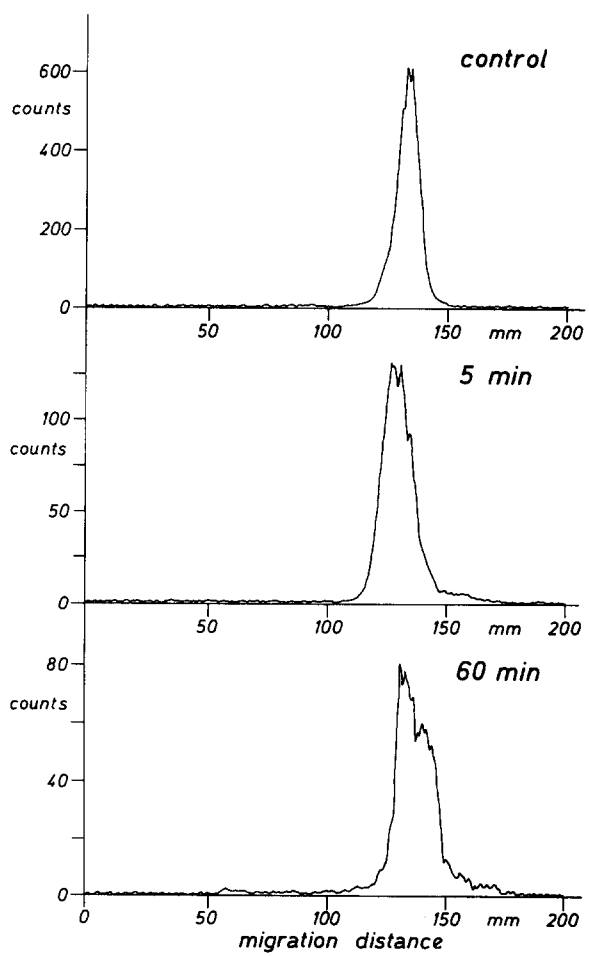

Fig. 3. Thin-layer chromatography of pravastatin. The supernatant of isolated rat liver cells incubated for 5 min and 60 min with 100 μM of radiolabelled pravastatin was chromatographed on thin-layer plates as described in Materials and Methods. Control = authentic drug. Radioactivity was detected using a radio-TLC analysator.

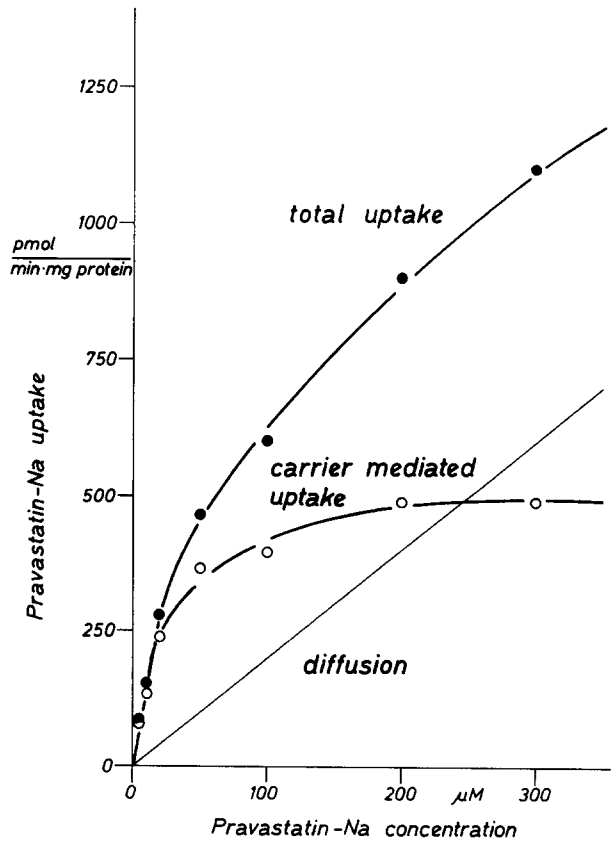

Fig. 4. Kinetics of the uptake of pravastatin into isolated rat hepatocytes. Aliquots of 1 ml of the hepatocyte suspension were incubated with 3.4 μM of radiolabelled pravastatin and different concentrations of unlabelled pravastatin. Initial uptake rates were calculated during the linear part of uptake. Uptake was measured at 37°C (●). Diffusion (–) and carrier-mediated uptake (○) were calculated using the program BMDPAR on a Cyber 960 computer. $n = 4$.

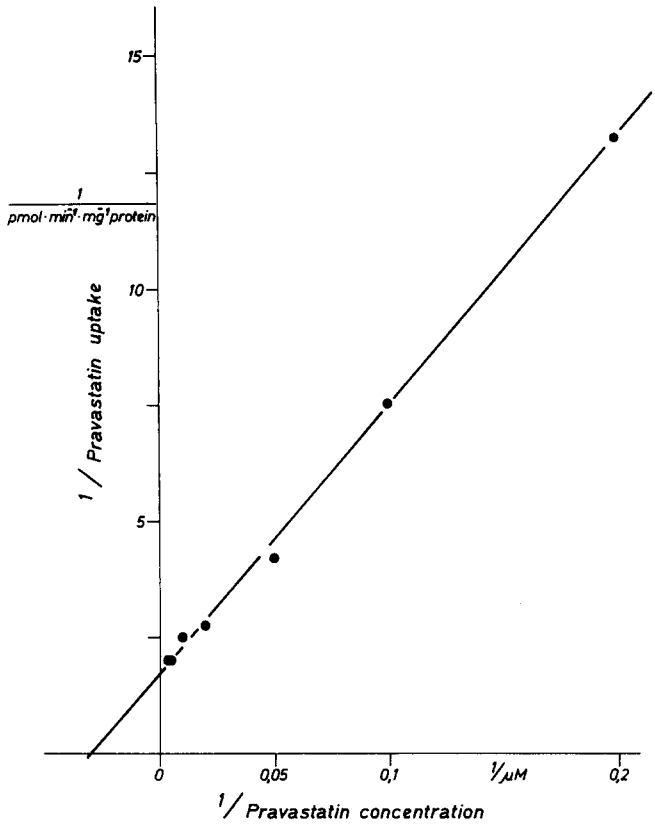

Fig. 5. Lineweaver-Burk plot of the carrier-mediated uptake of pravastatin. The initial uptake rates of the carrier-mediated uptake and the substrate concentrations were plotted according to Lineweaver and Burk. $K_m \approx 30$ µM, $V_{max} \approx 600$ pmol/mg per min.

Woolf-Hofstee plot one saturable transport system is responsible for the uptake of pravastatin-lactone (Fig. 10A,B).

Energy dependence of pravastatin and pravastatin-lactone uptake

After preincubation of liver cells with metabolic inhibitors, which decrease the cellular ATP-content by

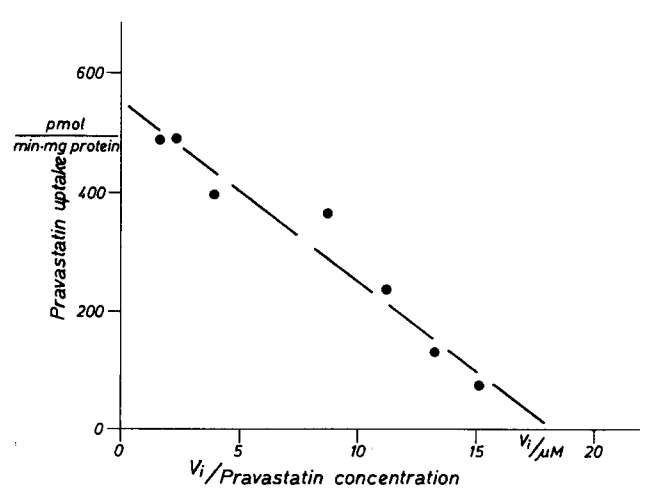

Fig. 6. Woolf-Hofstee plot of the carrier-mediated uptake of pravastatin. The data of Fig. 4 were plotted according to Woolf-Hofstee.

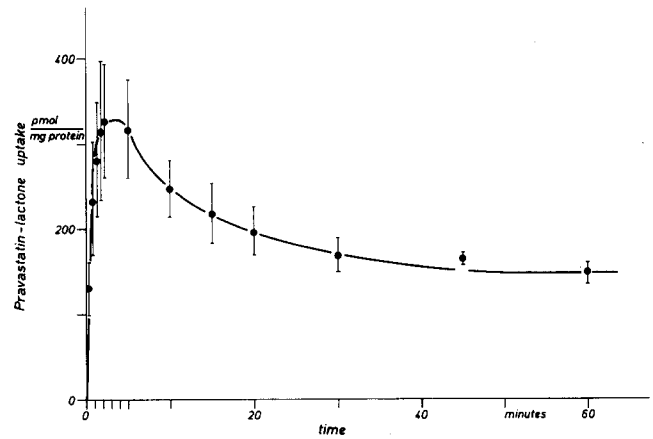

Fig. 7. Time dependence of the uptake of pravastatin-lactone into isolated rat hepatocytes. The uptake of 135 µM of a mixture of radiolabelled and unlabelled pravastatin-lactone was measured into isolated rat hepatocytes at 37°C as described in Materials and Methods.

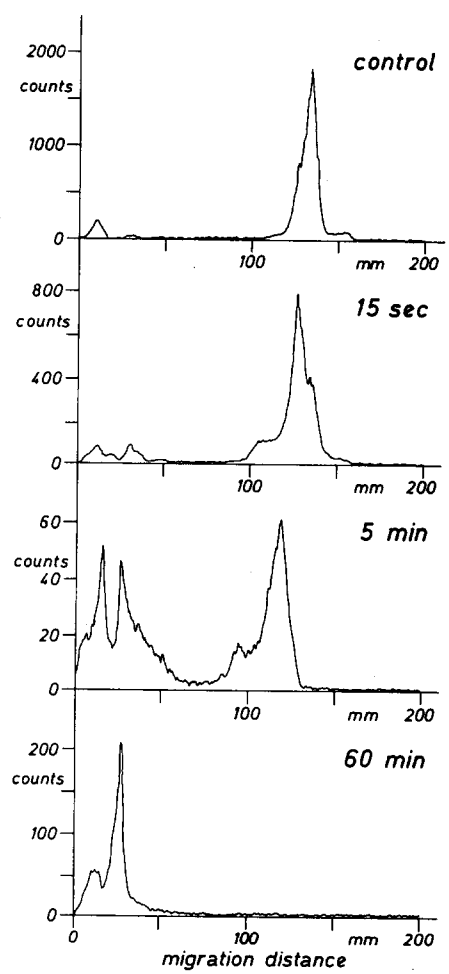

Fig. 8. Thin-layer chromatography of pravastatin-lactone. Isolated rat liver cells were incubated for 15 s, 5 and 60 min with radiolabelled pravastatin-lactone. Control = authentic drug. The supernatant of the cell suspension was analysed by thin-layer chromatography as described in Materials and Methods.

interferring with different targets in the respiratory chain, pravastatin uptake is inhibited. The same is true for pravastatin-lactone (Fig. 11A,B).

Incubation of liver cells for 30 min with N_2/CO_2 results in a 70% reduction of pravastatin and 75% reduction in pravastatin-lactone uptake. Transport could be restored by up to 80% by reoxygenation. (data not shown). Transport of pravastatin is temperature dependent (Fig. 12A). Q_{10} values are between 1.7 and 2.8. An apparent activation energy of 60 kJ/mol could by calculated for pravastatin uptake according to Arrhenius (Fig. 12B).

Only living cells are able to transport pravastatin and pravastatin-lactone. Dead cells with a permeabilized plasma membrane, as shown by Trypan blue inclusion, do not accumulate the HMG-CoA reductase inhibitors (Fig. 12A,B).

Driving forces of the uptake of pravastatin and pravastatin-lactone

The role of the sodium gradient as a possible driving force for pravastatin uptake was investigated in isolated hepatocytes which were suspended in sodium-free Tyrode buffer. Substitution of sodium by choline, lithium, potassium or *N*-methylglucamine had no significant effects on the uptake of pravastatin into isolated rat liver cells (Fig. 13).

The effect of variations of the membrane potential on the uptake of pravastatin was evaluated by anion-exchange studies. Chloride in the Tyrode buffer was

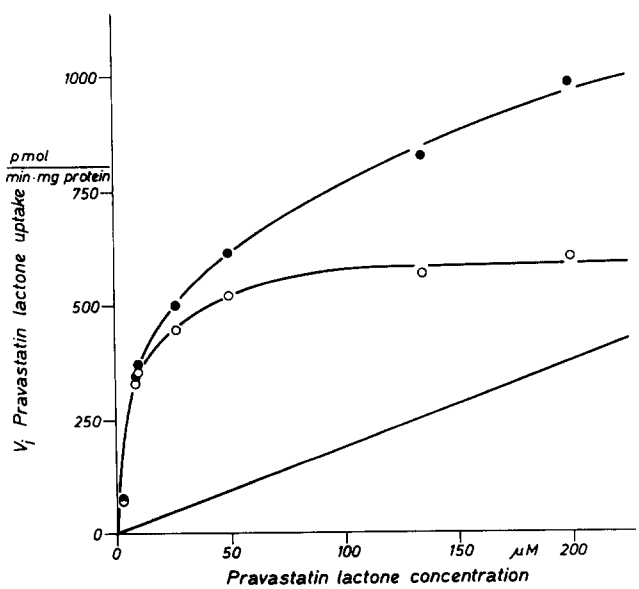

Fig. 9. Kinetics of the uptake of pravastatin-lactone into isolated rat liver cells. 1 ml of cell suspension was incubated with 2.7 µM of radiolabelled pravastatin-lactone and different concentrations of unlabelled compound. Uptake was measured at 37°C (•) and the initial uptake rates were calculated. Diffusion (–) and the carrier mediated uptake were calculated by computer (○) analysis. $n = 3$.

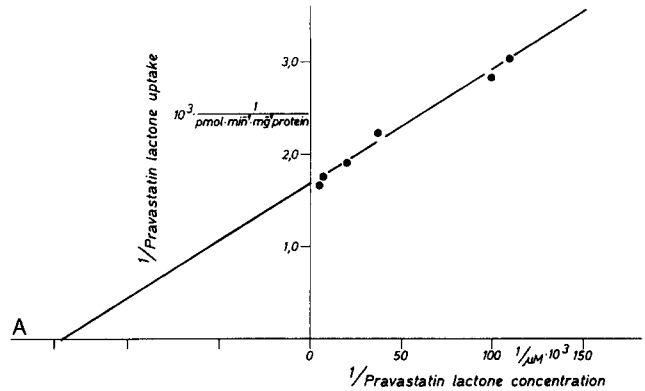

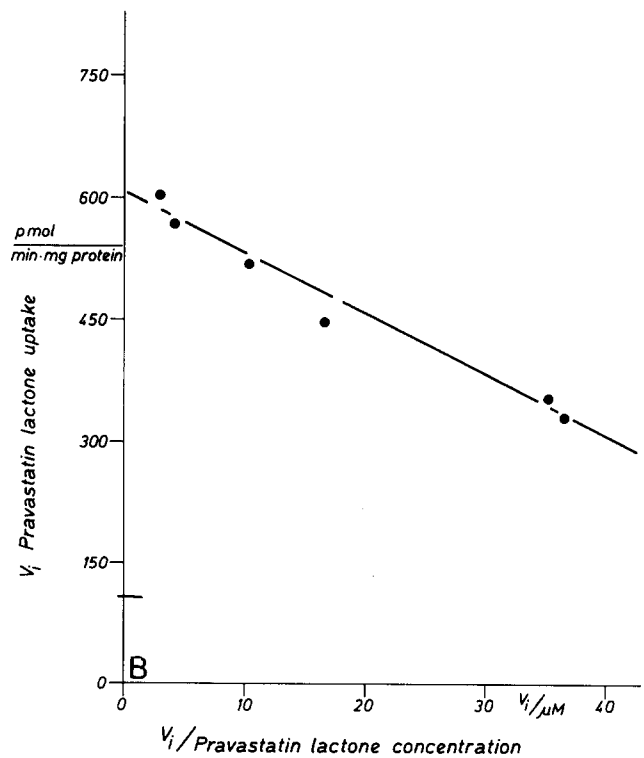

Fig. 10. Lineweaver-Burk (A) and Woolf-Hofstee (B) plot of the carrier-mediated uptake of pravastatin-lactone. The data in Fig. 9 were plotted according to Lineweaver and Burk and Woolf-Hofstee. $K_m \approx 10$ µM; $V_{max} \approx 650$ pmol/mg per min.

replaced by nitrate, sulfate, thiocyanate and gluconate. The lipophilic anions nitrate and thiocyanate generate a transient negative diffusion potential, whereas the slowly permeating sulfate and gluconate ions make the inner side of the membrane more positive in comparison to cells in normal Tyrode buffer [34]. Replacing chloride in the Tyrode buffer by the anions mentioned above leads to a significant inhibition of pravastatin uptake (Fig. 14).

Studies on the evaluation of the endogenous substrates of the pravastatin carrier

In a previous study we found that pravastatin competitively inhibits the uptake of cholate and tauro-

cholate in a sodium-free buffer [21]. In contrast, the sodium-taurocholate cotransporter was not influenced by pravastatin in micromolar concentrations. In addition, all other known endogenous transport systems in rat liver cells were also not inhibited by pravastatin [21]. This prompted us to speculate that a sodium-independent bile acid carrier is responsible for the hepatoselective uptake of pravastatin [21,22]. To verify this hypothesis mutual inhibition studies were performed. Cholate and taurocholate competitively inhibit the uptake of pravastatin in the presence and absence of sodium (Table I). The K_i values are 22 ± 2 μM for cholate in the presence of sodium and 45 ± 4 μM in the absence of sodium and 15 ± 5 μM and 35 ± 3 μM for taurocholate, respectively. For further characterization of the transporter, the influence of other anionic compounds such as BSP [35] and bumetanide [36] on pravastatin uptake was evaluated. In the absence of sodium, BSP and bumetanide competitively inhibit pravastatin uptake. The K_i values are 24 ± 1.5 μM for BSP and 62 ± 7 μM for bumetanide.

Since pravastatin-lactone is also taken up by hepatocytes by a carrier-mediated mechanism, mutual transport inhibition studies with pravastatin were performed. Pravastatin-lactone and pravastatin are mutual competitive-noncompetitive (mixed type of inhibition) transport inhibitors (Table I). Lovastatin, which is also administered as lactone, competitively-noncompetitively blocked (mixed type of inhibition) the uptake of pravastatin-lactone and pravastatin (Table I).

Discussion

Two-thirds of the total cholesterol found in the body is of endogenous origin, with the major site of cholesterol biosynthesis being the liver [9]. Liver-derived cholesterol is the main cause for the development of hypercholesterolaemia, whereas cholesterol production in non-hepatic cells is needed for normal cell function [37,38]. Therefore, selective inhibition of HMG-CoA reductase in the liver is a major demand in the development of HMG-CoA reductase inhibitors. Preferential inhibition of sterol synthesis within the liver may minimize adverse effects in cholesterol-dependent non-hepatic tissues. Pravastatin is one of the most liver-selective HMG-CoA-reductase inhibitors yet developed [12]. Pravastatin has a dihydroxy heptanoic acid function, which resembles the HMG moiety of HMG-CoA. It is administered in its open acid form, whereas simvastatin and lovastatin are administered as lactones and hydrolysis to the active acid form occurs in the liver [20]. Pravastatin, which is a hydroxy derivative of mevastatin, differs from all other inhibitors in its physicochemical properties. Pravastatin is hydrophilic and this feature is thought to be responsible for its hepatoselectivity [6]. In several studies it was

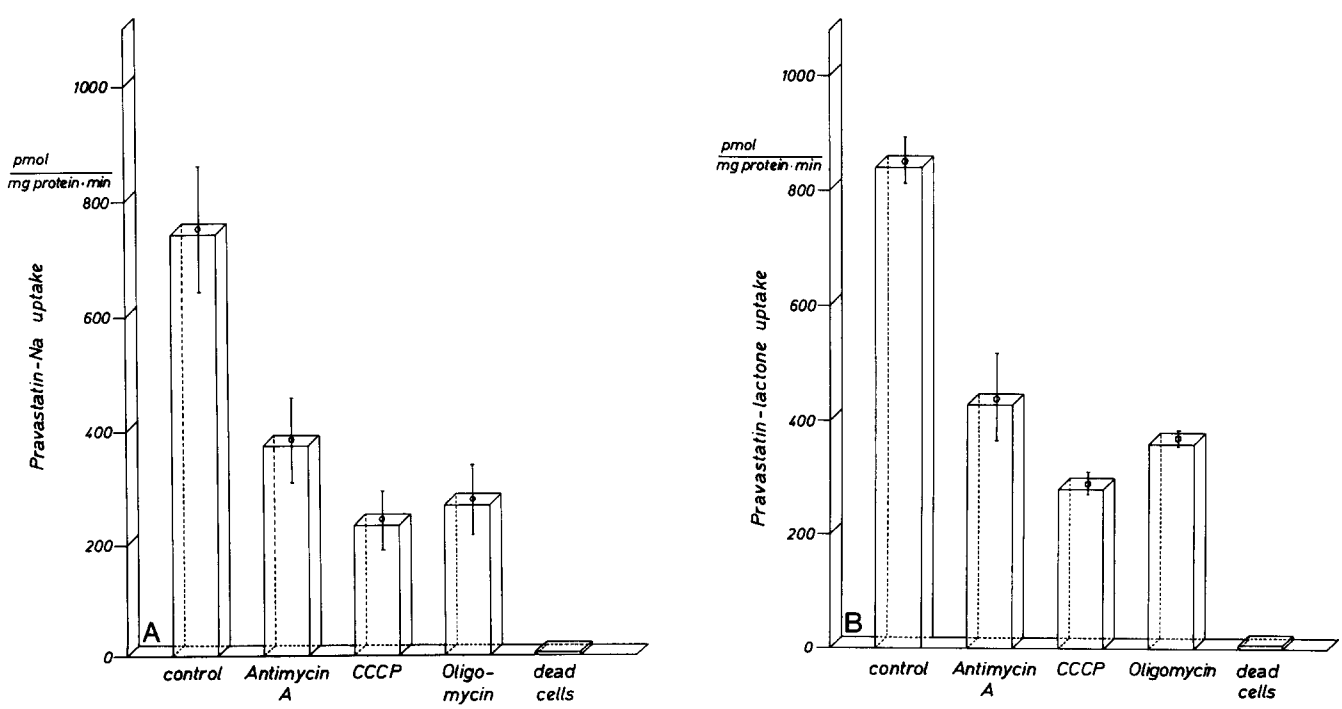

Fig. 11. Uptake of pravastatin (A) and pravastatin-lactone (B) in the presence of metabolic inhibitors and into dead cells. Aliquots of 1 ml liver cells were incubated for 10 min with 10 μg/ml antimycin A, 4 μg/ml CCCP, 10 μg/ml oligomycin prior to the addition of 100 μM pravastatin or 135 μM of pravastatin-lactone. Initial uptake rates were measured. Dead hepatocytes were produced by freezing the cells in liquid nitrogen and slowly thawing at room temperature. 100% of the cells took up the dye Trypan blue. $n = 4$; means $\pm$ S.D.; $P < 0.001$.

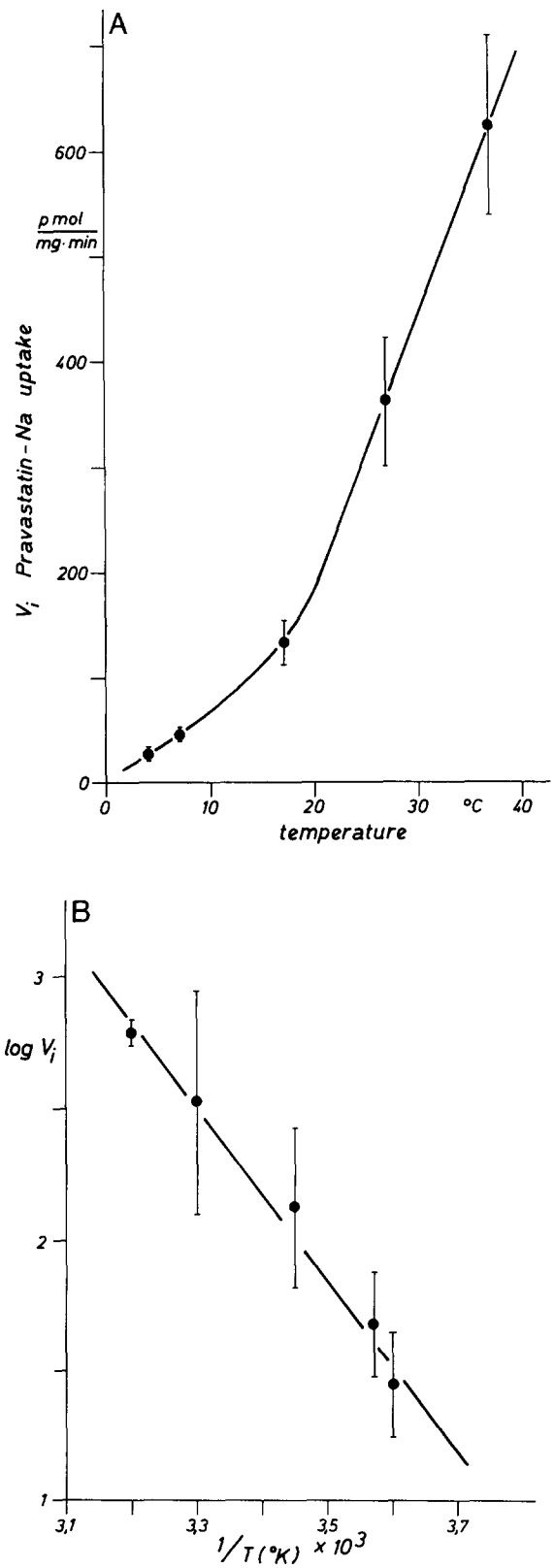

Fig. 12. Temperature dependence of the uptake of pravastatin (A) and Arrhenius diagram of the data (B). The uptake of 100 μM of a mixture of radiolabelled and unlabelled pravastatin was measured into isolated hepatocytes at 4, 7, 17, 27 and 37°C. Initial uptake rates were calculated (A) and plotted according to Arrhenius (B). $n = 3$; means ± S.D.

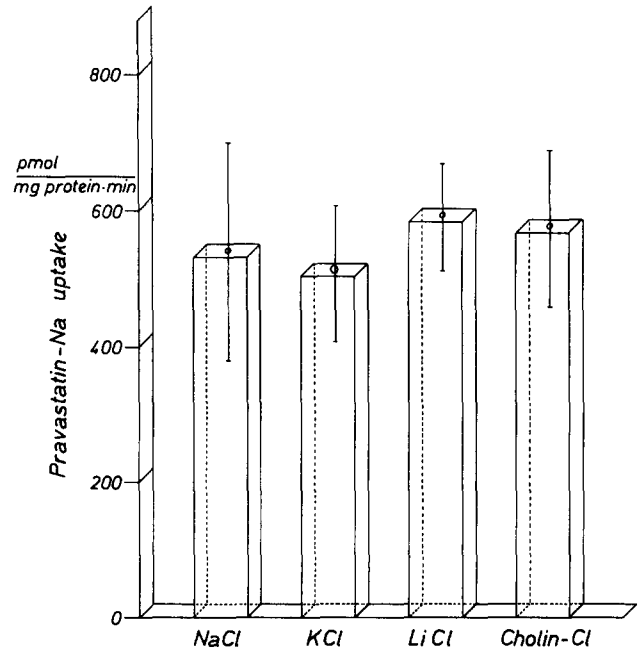

Fig. 13. Sodium dependence of pravastatin uptake. The uptake of pravastatin was measured in Tyrode buffer in which sodium was replaced by lithium, potassium and choline. Initial uptake rates were measured. $n = 4$; means ± S.D.

shown that pravastatin in contrast to simvastatin or lovastatin does not penetrate into non-hepatic tissues [4–6] but could enter hepatocytes effectively [39]. Side effects such as decrease of the replicative capacity of endothelial cells, smooth muscle cells and fibroblasts were seen using lovastatin [40] whereas pravastatin did

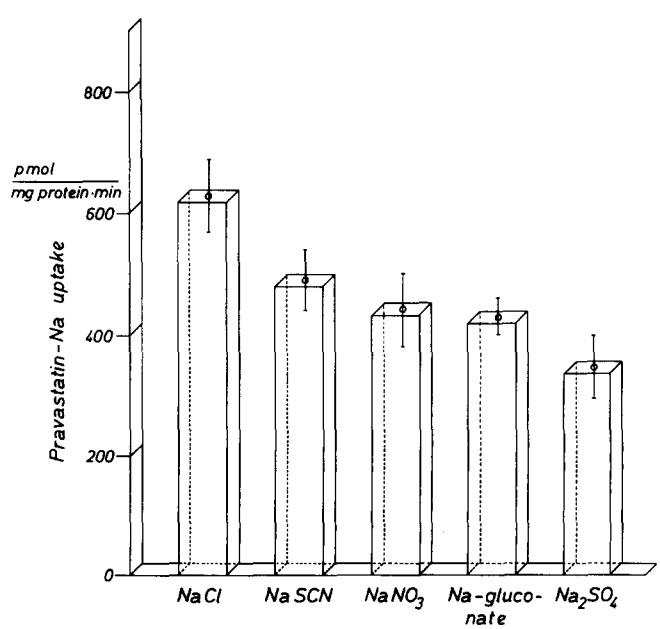

Fig. 14. Chloride dependence of pravastatin uptake. The uptake of pravastatin was measured in Tyrode buffer in which chloride was replaced by nitrate, sulfate, thiocyanate and gluconate. Initial uptake rates were measured. $n = 4$; means ± S.D.; $P < 0.01$.

TABLE I

Kinetic data of the transport of pravastatin or pravastatin-lactone in the presence of bile acids, bumetanide, BSP, lovastatin, pravastatin and pravastatin-lactone

The initial uptake rates of increasing concentrations of pravastatin or pravastatin-lactone were measured 30 s after addition of four increasing concentrations of cholate, taurocholate, BSP, bumetanide, pravastatin and pravastatin-lactone either in sodium-Tyrode buffer or sodium-free-Tyrode buffer (sodium was replaced by choline). Data were plotted according to Cornish-Bowden [31] and Dixon [32].

(A) Studies in sodium-Tyrode buffer

(i) Substrate pravastatin

Inhibitor	K_i (μM)	Type of inhibition
Cholate	22±2	competitive
Taurocholate	15±5	competitive

(B) Studies in the absence of sodium

(i) Substrate pravastatin

Inhibitor	K_i (μM)	Type of inhibition
Cholate	45±4	competitive
Taurocholate	35±3	competitive
BSP	24±1.5	competitive
Bumetanide	62±7	competitive
Pravastatin-lactone		mixed competitive/noncomp.
Lovastatin		mixed competitive/noncomp.

(ii) Substrate pravastatin-lactone

Inhibitor	K_i (μM)	Type of inhibition
Pravastatin		mixed competitive/noncomp.
Lovastatin		mixed competitive/noncomp.

not inhibit sterol sysnthesis in the lens [11]. In a former study in 1992 [21] we looked for the reason of the hepatoselectivity of pravastatin and found that pravastatin has a high affinity to a sodium-independent bile acid carrier [21]. This transport system exists predominantly in liver cells [22], but is not found in non-hepatic tissues such as fibroblasts. In the study presented we evaluated the cell specificity and characterized the hepatocellular uptake mechanisms of pravastatin and pravastatin-lactone in more detail.

Pravastatin and pravastatin-lactone uptake is liver-cell specific. No other cell types tested e.g. AS 30D ascites hepatoma cells or FAO cells accumulate either compound as much as hepatocytes do. This is in agreement with studies of Shaw et al. [41] who showed that pravastatin is a weak inhibitor of sterol synthesis in hepatoma cells [41]. The cell specificity of pravastatin compared to lovastatin or simvastatin is not dependent on the open acid form since also the lactone form of pravastatin enters liver cells. The most important structural difference between pravastatin and lovastatin, which seems to be responsible for hepatoselectivity, is the hydroxyl group at the 6-position of the ring system. Further studies on the structure–activity relationship and comparison with the structure of the physiological substrate of the carrier (cholate 21) will be needed to obtain a clear picture of the structural requirements for transport into liver cells.

Pravastatin and pravastatin-lactone uptake into isolated rat liver cells is carrier mediated. This was confirmed by the following:

(1) Saturation kinetics with respect to substrate concentration. Pravastatin and pravastatin-lactone are taken up by one saturable transport protein. The K_m values are in the range of that found for the sodium-independent bile acid carrier [42]. The affinity of pravastatin to the transport protein is 3-fold lower compared with that of the lactone. This may be due to the somewhat higher lipophilicity of the lactone which enables a better penetration of the compound into the lipid bilayer. At higher concentrations part of the uptake is due to non-ionic diffusion. This is a phenomenon which has been already demonstrated for other substrates of hepatocellular transport systems [22,28,36]. Permeability coefficients increased with increasing temperature. The permeability coefficient of $5.8 \cdot 10^{-6}$ (pravastatin) and $5.4 \cdot 10^{-6}$ cm/s (pravastatin-lactone) at 37°C is low, which would be expected for a hydrophilic compound and has been also found for other hydrophilic compounds [22,28,43]. For hydrophobic compounds permeability coefficients in the range of $1–3 \cdot 10^{-4}$ cm/s have been determined [44].

(2) Energy dependence. Transport is blocked by lowering the intracellular ATP content. At present, however, the exact driving forces for the uptake are not known. Pravastatin uptake is neither driven by the sodium gradient nor by the membrane potential. Transport seems to be dependent on the presence of chloride anions, since replacement of chloride by sulfate, nitrate, thiocyanate and gluconate leads to a reduced uptake. These anions lead to de- or hyperpolarization of the membrane potential. Since pravastatin is anionic under physiological conditions, a more positive membrane potential could be a driving force for the uptake. But this was not the case. Pravastatin uptake was reduced when chloride ions were missing. This result is not in agreement with the result of a study on pravastatin uptake published recently [45] in which chloride was only replaced by gluconate. The reason for this is unknown at present but may be due to different experimental conditions. Inhibitory effects of chloride replacement were also found for the uptake of cholate [22], BSP [46] and taurocholate [47]. In the case of BSP and cholate a clear picture of the driving forces and the importance of the chloride ion in the transport process has not been drawn. Therefore additional studies in isolated membrane vesicles are needed to characterize the driving forces for pravastatin uptake.

(3) Temperature dependence. Q_{10} values between 1.7 and 2.8 and an activation energy of 60 kJ/mol are indicative for protein-mediated uptake.

(4) Concentrative transport (uphill transport). Pravastatin and pravastatin-lactone are accumulated several fold over the extracellular concentration into liver cells. This is indicative for an active transport system which is only operating in intact cells. The importance of intracellular binding proteins for the uptake of pravastatin and pravastatin-lactone was ruled out using permeabilized liver cells. In these cells uptake of both compounds was negligible. In addition, 90% of the accumulated pravastatin is found in the cytosol and not bound to cellular membranes. Only 10% of the compound is associated with the membrane fraction.

After 30 min of incubation of liver cells with pravastatin-sodium, a steady-state in uptake is reached. This is in contrast to the uptake of pravastatin-lactone. After 5 min of incubation with the lactone, cell-associated compound decreases. This prompted us to analyze the occurrence of possible metabolites of pravastatin-lactone in the supernatant of liver cells. Whereas the native compound was found in the supernatant of cells preincubated with pravastatin-sodium, metabolites were detected after 5 and 60 min of incubation of the cells with pravastatin-lactone. The structure of the metabolites of the lactone are precently not known. The decrease of pravastatin-lactone in the hepatocytes, however, corresponds with the increase of the metabolite in the supernatant.

(5) Substrate specificity of uptake. Transport of pravastatin and pravastatin-lactone is competitively inhibited by cholate and taurocholate. As was shown in 1992 already [21], pravastatin inhibits the sodium-independent uptake of cholate and taurocholate in a competitive manner, whereas the sodium-taurocholate transporter is influenced by pravastatin in millimolar concentrations only. Since the therapeutic concentrations of pravastatin are in the nanomolar range the sodium-taurocholate cotransporter can not be responsible for hepatocellular uptake of pravastatin. On the other hand, the mutual competitive transport inhibition of bile acids and pravastatin and pravastatin-lactone in sodium-free medium indicates that these compounds share a common transport system.

Although bumetanide, an anionic loop-diuretic [36], competitively inhibited the uptake of pravastatin it doesn't seem to be a substrate of the carrier since in mutual transport inhibition studies pravastatatin noncompetitively inhibited bumetanide uptake [21]. BSP, another anionic compound, which seems to be transported at least via three different transport systems [35], competitively inhibits pravastatin uptake. Measuring the overall transport of BSP in isolated hepatocytes, pravastatin competitively blocked BSP uptake. Under physiological conditions BSP is highly albumin bound. Our studies were done in albumin free buffers, therefore additional experiments in the presence of albumin have to be performed before an assignment of the pravastatin carrier to one of the BSP carrier can be done.

The more lipophilic HMG-CoA-reductase inhibitor lovastatin in its lactone form inhibited the uptake of pravastatin and pravastatin-lactone. Kinetic evaluations showed a mixed (competitive/noncompetitive) type of inhibition. The same is true for the mutual transport inhibition of pravastatin and pravastatin-lactone. This was unexpected since lovastatin in its open acid form has been shown to competitively inhibit pravastatin uptake [45]. It seems that the compounds do not only interact with the substrate binding site of the protein but also with other parts of the transport protein leading to conformational changes. To further elucidate this phenomenon and to characterize the driving forces and the involvement of one of the BSP carriers in pravastatin and pravastatin-lactone uptake, studies with isolated basolateral plasmamembrane vesicles are currently performed in our laboratory.

Acknowledgments

The authors thank Dr. B. Boschek for critically reading the manuscript, Dr. M. Krekler and Dr. R. Gregg (Bristol-Myers Squibb) for valuable discussion and providing the HMG-CoA reductase inhibitors.

References

1 Illingworth, D.R. (1991) Drugs 41, 151–160.
2 Kathawala, F.G. (1991) Med. Res. Rev. 11, 121–146.
3 Aronson, J.K. and Leong, L. (1990) Q.J. Med. 74, 111–115.
4 Tsujita Y. and Watanabe Y. (1986) Cardiovasc. Drug Rev. 7, 110–126.
5 Tsujita, Y., Kuroda, M., Shimada, Y., Tanzawa, K., Arai, M., Kaneko, K., Tanaka, M., Masuda, H., Tarumi, C., Watanabe, Y. and Fujii, S. (1986) Biochim. Biophys. Acta 877, 50–60.
6 Scott, W.A.(1990) Lipid Management, Round Table Series 16, 17–25.
7 Alberts, A.W. (1988) Am. J. Cardiol. 62, 10J–15J.
8 Tobert, J.A., Shear, C.L., Chremos, A.N. and Mantel, G.E. (1990) Am. J. Cardiol. 65, 23F–26F.
9 Brown, M.S. and Goldstein, J.L. (1983) J. Clin. Invest. 72, 743–747.
10 Parker, R.A., Clark, R.W., Sit, S.Y., Lanier, T.L., Grosso, R.A. and Wright, J.J.K. (1990) J. Lipid Res. 31, 1271–1282.
11 Mosley, S.T., Kalinowski, S.S., Schafer, B.L. and Tanaka, R.D. (1989) J. Lipid Res. 30, 1411–1420.
12 Bocan, T.M.A., Ferguson, E., McNally, W., Uhlendorf, P.D., Mueller, S.B., Dehart, P., Sliskovic, D.R., Roth, B.C., Krause, B.R. and Newton, R.S. (1992) Biochim. Biophys. Acta 1123, 133–144.
13 Koga, T., Shimada, Y., Kuroda, M., Tsujita, Y., Hasegawa, K. and Yamazaki, M. (1990) Biochim. Biophys. Acta 1045, 115–120.
14 Germershausen, J.I., Hunt, V.M., Bostedor, R.G., Bailey, P.J., Karkas, J.D. and Alberts, A.W. (1989) Biochem. Biophys. Res. Commun. 158, 667–675.
15 Krukemyer, J.J. and Talbert, R.L. (1987) Pharmacotherapy 7, 198–210.
16 Tobert, J.A. (1987) Circulation 76, 534–538.

17 MacDonald, J.S., Gerson, R.J., Kornbrust, D.J., Kloss, M. W., Prahalada, S., Berry, P.H., Alberts, A.W. and Bokelman, D.L. (1988) Am. J. Cardiol. 62, 16J–27J.
18 Scott, W.A., Mahoney, E.M. and Mosley, S.T. (1989) in New Advances in the Control of Lipid Metabolism: Focus on Pravastatin (La Rosa, J.C., ed.), pp. 1–8, Royal Society of Medicine Services International Congress and Symposium Series.
19 Watanabe, H. (1990) Annu. Rep. Sankyo Res. Lab. 42, 117–120.
20 Pan, H.Y., DeVault, R.A., Wang-Iverson, D., Ivashkiv, E., Swanson, B.N. and Sugerman, A. (1990) J. Clin. Pharmacol. 30, 1128–1135.
21 Ziegler, K. and Stünkel, W. (1992) Biochim. Biophys. Acta 1139, 203–209.
22 Frimmer, M. and Ziegler, K. (1988) Biochim. Biophys. Acta 947, 75–99.
23 Hummelsiep, S. Ziegler, K. (1992) Biol. Chem. Hoppe-Seyler 373, 780.
24 Berry, M.N. and Friend, D.S. (1969) J. Cell Physiol. 43, 506–520.
25 Baur, H., Kasparek, S. and Pfaff, E. (1975) Hoppe-Seyler's Z. Physiol. Chem. 356, 827–838.
26 Bradford, M. (1976) Anal. Biochem. 72, 248–254.
27 Klingenberg, M. and Pfaff, E. (1967) Methods Enzymol. 10, 680–684.
28 Bertrams, A.A. and Ziegler, K. (1991) Biochim. Biophys. Acta 1091, 337–348.
29 Lineweaver, H. and Burk, D. (1934) J. Am. Chem. Soc. 56, 658–666.
30 Hofstee, B.H.J. (1959) Nature 184, 1296–1298.
31 Cornish-Bowden, A. (1974) Biochem. J. 137, 143–144.
32 Dixon, M. (1953) Biochem. J. 55, 170–171.
33 Kroker, R., Anwer, M.S. and Hegner, D. (1978) Naunyn-Schmiedeberg's Arch. Pharmacol. 303, 299–301.
34 Fitz, J.G., Bass, N.M. and Weisinger, R.A. (1991) Am. J. Physiol. 261, G83–G91.
35 Tiribelli, C., Lunazzi, G.C. and Sottocasa, G.L. (1990) Biochim. Biophys. Acta 1031, 261–275.
36 Petzinger, E., Müller, N., Föllmann, W., Deutscher, J. and Kinne, R.K.H. (1989) Am. J. Physiol. 256, G78–G86.
37 Kannel, W.B., Castelli, W.P. and Gordon, T. (1979) Ann. Intern. Med. 90, 85–91.
38 Sinensky, M. and Logel, J. (1985) Proc. Natl. Acad. Sci. USA 82, 3257–3261.
39 Komai, T., Shigehara, E., Tokui, T., Koga, T., Ishigami, M., Kuroiwa, C. and Horiuchi, S. (1992) Biochem. Pharmacol. 43, 667–670.
40 Falke, P.I., Mattiasson, L., Stavenow, L. and Hood, B. (1989) Pharmacol. Toxicol. 64, 173–176.
41 Shaw, M.K., Newton, R.S., Sliskovic, D.R., Roth, B.D., Ferguson, E. and Krause, B.R. (1990) Biochem. Biophys. Res. Commun. 170, 726–734.
42 Anwer, M.S. and Hegner, D. (1978) Naunyn-Schmiedeberg's Arch. Pharmacol. 359, 181–192.
43 Ziegler, K. and Seeberger, A. (1993) Biochem. Pharmacol. 45, 909–916.
44 Ziegler, K., Polzin, G. and Frimmer. M. (1988) Biochim. Biophys. Acta 938, 44–50.
45 Yamazaki, M., Suzuki, H., Hanano, M., Tokui, T., Komai, T. and Sugiyama, Y. (1993) Am. J. Physiol. 264, G36–G44.
46 Wolkoff, A.W., Samuelson, A.C., Johansen, K.L., Nakata, R., Withers, D.M. and Sosiak, A. (1987) J. Clin. Invest. 79, 1259–1268.
47 Meier, P.J., Meier-Abt, A.St., Barrett, C. and Boyer, J.L. (1984) J. Biol. Chem. 259, 10614–10622.